

# UC Irvine

## UC Irvine Previously Published Works

### Title

Wide-field Hemodynamic Neuroimaging of Rodents using a Modified openSFDI Build

### Permalink

<https://escholarship.org/uc/item/7b36b103>

### Authors

Phan, T

Crouzet, C

Kennedy, GT

[et al.](#)

### Publication Date

2022

### Copyright Information

This work is made available under the terms of a Creative Commons Attribution License, available at <https://creativecommons.org/licenses/by/4.0/>

Peer reviewed

# Wide-field Hemodynamic Neuroimaging of Rodents using a Modified openSFDI Build

Thinh Phan<sup>1,2</sup>, Christian Crouzet<sup>1,2</sup>, Gordon T. Kennedy<sup>1</sup>, Anthony J. Durkin<sup>1,2</sup>, Bernard Choi<sup>1,2,3,4,\*</sup>

<sup>1</sup>Beckman Laser Institute and Medical Clinic, University of California, Irvine, 1002 Health Sciences Road East, Irvine, CA 92612, USA

<sup>2</sup>Department of Biomedical Engineering, University of California, Irvine, 3120 Natural Sciences II, Irvine, CA 92697, USA

<sup>3</sup>Edwards Lifesciences Foundation Cardiovascular Innovation Research Center, University of California, Irvine, 2400 Engineering Hall, Irvine, CA 92697, USA

<sup>4</sup>Department of Surgery, University of California, Irvine, 333 City Boulevard West, Suite 1600, Orange, CA 92868, USA

\*Corresponding author's contact: choib@uci.edu

**Abstract:** We modified and combined an open-source spatial frequency domain imaging (openSFDI) build with laser speckle imaging (LSI) into a widefield rodent cortical hemodynamic imaging system. Here, we present system specifications and in-vitro phantom measurement results. © 2022 The Author(s)

## Introduction

Spatial frequency domain imaging (SFDI) is a diffuse optical imaging technique that utilizes structured illumination to quantify tissue's optical properties, specifically absorption ( $\mu_a$ ) and reduced scattering ( $\mu_s'$ ) coefficients. In comparison to point-based diffuse optical methods (e.g., near-infrared spectroscopy), SFDI offers mapping of optical properties, and subsequently concentrations of hemoglobin (HbR) and deoxy-hemoglobin (HbO<sub>2</sub>) and physiologically relevant parameters such as oxygen saturation (StO<sub>2</sub>). Recent studies have employed SFDI to image wounds and wound healing processes such as burns, skin graft, and diabetic foot ulcers [1,2].

However, SFDI utilization in neuroimaging has been limited. A few notable studies used SFDI to measure in-vivo optical properties and cortical hemodynamics of rodents, often through a cranial window prep. These studies mainly aimed to quantify changes in optical properties and hemodynamic responses to specific brain-related diseases such as epilepsy, migraine, ischemic stroke, and Alzheimer's disease [3-6]. More information regarding these studies can be found in a recent review paper on SFDI by Gioux *et al.* [7].

Previously, we reported on a multimodal mesoscopic imaging system combining SFDI and laser speckle imaging (LSI) for rodents [8]. This system enabled fast (14 Hz for SFDI, 60 Hz for LSI) imaging of cerebral hemodynamics during cardiac arrest and resuscitation. Here, we describe a small-animal wide-field optical neuroimager build based on the openSFDI platform described by Applegate *et al.* [9]. This system incorporates LSI as a second modality with a co-registered FOV (10mm x 10mm) with the SFDI images, facilitating the quantitative mapping of the cortical hemodynamics with measurements of HbR, HbO<sub>2</sub>, StO<sub>2</sub>, and cerebral blood flow. Below, we describe system specifications and performance characterization measurements using silicone phantoms.

## Methods and Results

### 1) System design specifications:

The SFDI design (Fig. 1A) is adapted from the openSFDI build guide with a few modifications. The illumination setup includes mounted LED modules from Thorlabs at 660, 780, and 850 nm (M660L4, M780LP1, M850L3, and LEDD1B, Thorlabs, NJ, USA) and appropriate dichroic mirrors. In addition, we utilized a long-coherence-length 633 nm laser (SureLock RO, Coherent, CA, USA) for LSI illumination, with laser light expanded using an aspheric lens and homogenized using a diffuser. To achieve similar FOVs for both modalities, we used the same CMOS cameras (BFS-U3-32S4M-C, FLIR, OR, USA) and lens (50mm VIS-NIR #67-717, Edmund Optics, NJ, USA) combinations for both SFDI and LSI. Here, a dichroic mirror, lens spacers, and notch and line filters were also used to ensure that both cameras have similar FOVs of ~10 mm x 10 mm with 1200 x 1200 pixel resolution, which is a typical size of a mouse cranial window preparation.

We used an Arduino UNO (Rev3, Arduino, MA, USA) to trigger the DMD (LC4500-NIR-EKT, Keynote Photonics, TX, USA) and LED light sources. The output signal from the DMD is then used to trigger the camera's acquisition. The computer is the master controller that starts and stops the Arduino's triggering sequence using LabVIEW (LabVIEW 2020 64-bit, NI, TX, USA) through serial communication. We chose a 10 ms exposure time for both the DMD and the cameras with a delay of 10 ms to avoid dropping frames. The detailed triggering schematic

can be found below in Fig 1B. The system can currently achieve a 50 Hz total frame rate with minimal dropped frames (1 in 15000 frames), resulting in an effective  $\sim 2.78$  Hz for SFDI (at two spatial frequencies with 3 phases: 0 and  $0.3 \text{ mm}^{-1}$ ) and 50Hz for LSI.

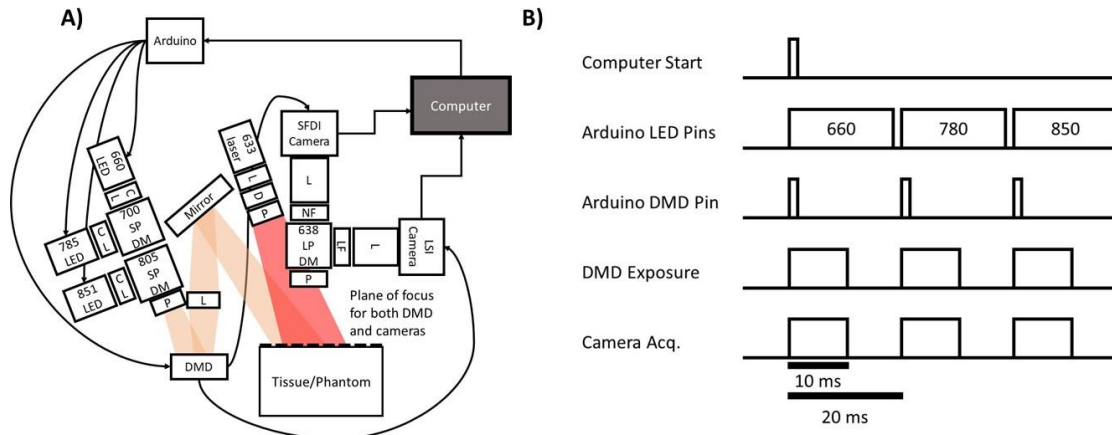


Fig 1. A) Design of the system and B) its triggering scheme.

## 2) Phantom measurements:

We performed a comparison study with a commercial SFDI (Reflect RS, Modulim, CA, USA) device using four silicone phantoms made in-house, imaged at 0 and  $0.3 \text{ mm}^{-1}$  spatial frequencies. Results for 660 and 850 nm are shown below in Fig 2. The neuroimaging system in its current state can achieve a high correlation with a commercial device ( $R^2 = 0.99$ ). The percentage error for  $\mu_a$  ranges from -20.0 to -1.4% (or -0.0061 to -0.00032  $\text{mm}^{-1}$ ), while that of  $\mu_s'$  ranges from 0.8 to 7.0% (or 0.019 to 0.12  $\text{mm}^{-1}$ ). Note that for  $\mu_a$ , the percent error is largest at low  $\mu_a$  values.

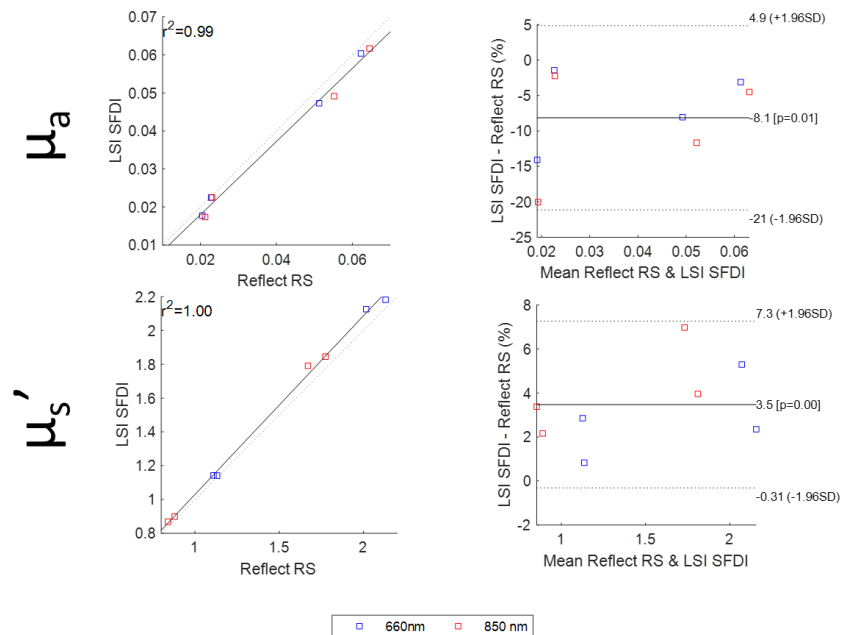


Fig 2. Phantom measurements comparison with a commercial SFDI device at 660 and 850 nm. Correlation and Bland-Altman plots are displayed from left to right, respectively.

## References

- [1] G.T. Kennedy *et al.*, "Spatial frequency domain imaging: a quantitative, noninvasive tool for in vivo monitoring of burn wound and skin graft healing" in *J Biomed Opt* **24**(7), 071615 (2019).
- [2] S. Lee *et al.*, "SFDI biomarkers provide a quantitative ulcer risk metric and can be used to predict diabetic foot ulcer onset" in *J Diabetes Complicat* **34**(9), 107624 (2020).
- [3] D. Abookasis *et al.*, "Imaging cortical absorption, scattering, and hemodynamic response during ischemic stroke using spatially modulated near-infrared illumination" in *J. Biomed. Opt.*, **14**(2), 024033 (2009).

- [4] O. Shaul *et al.*, “Application of spatially modulated near-infrared structured light to study changes in optical properties of mouse brain tissue during heatstress” in *Appl. Opt.*, **56**(32), 8880–8886 (2017).
- [5] A. J. Lin *et al.*, “Spatial frequency domain imaging of intrinsic optical property contrast in a mouse model of Alzheimer’s disease” in *Ann. Biomed. Eng.*, **39**(4), 1349–1357 (2011).
- [6] S. Sunil *et al.*, “Stroke core revealed by tissue scattering using spatial frequency domain imaging” in *Neuroimage-Clin.*, **29** 102539 (2021).
- [7] S. Gioux, A. Mazhar, D. J. Cuccia, “Spatial frequency domain imaging in 2019: principles, applications, and perspectives” in *J Biomed Opt* **24**(7), 071613 (2019).
- [8] R .H. Wilson *et al.*, “High-speed spatial frequency domain imaging of rat cortex detects dynamic optical and physiological properties following cardiac arrest and resuscitation” in *Neurophotonics* **4**(4), 045008 (2017).
- [9] M. B. Applegate *et al.*, “OpenSFDI: an open-source guide for constructing a spatial frequency domain imaging system” in *J Biomed Opt* **25**(1), 016002 (2020).